J. Membrane Biol. 100, 137–148 (1987)

The Journal of
Membrane Biology

Physiological Regulation of Transepithelial Impedance in the Intestinal Mucosa of Rats and Hamsters

J.R. Pappenheimer*
Department of Physiology and Biophysics, Harvard Medical School, Boston, Massachusetts 02115

Summary. Isolated intestinal segments from rats or hamsters were recirculated with balanced salt solutions containing fluorocarbon emulsion to provide 6 vpc oxygen. The lumen contained an axial Ag-AgCl electrode, and the serosal surface was surrounded by a cylindrical shell of Ag-AgCl. Transmural impedances were measured at frequencies from 0.01–30 kHz before and after removal of the mucosal epithelium. The resistance of intercellular junctions, R_J, the distributed resistance of the lateral spaces, R_L, and the distributed membrane capacitance, C_M, were computed from the relations between frequency and impedance. Activation of Na-coupled solute transport by addition of glucose, 3-0-methyl glucose, alanine or leucine caused two- to threefold decreases of transepithelial impedance. Typical changes induced by glucose in hamster small intestine were R_J 30 → 13 Ω, R_L 23 → 10 Ω, and C_M 8 → 20 μF (per cm length of segment). Half maximal response occurred at a glucose concentration of 2–3 mM. The area per unit path length of the junctions ($Ap/\Delta x$ = specific resistance ÷ R_J) in glucose activated epithelium was 3.7 cm in hamster midgut and 6.8 cm in rat. These values are close to the 4.3 cm estimated independently from coefficients of solvent drag and hydrodynamic conductance in glucose-activated rat intestine in vivo. The transepithelial impedance response to Na-coupled solute transport was reversibly dependent upon oxygen tension.

It is proposed that activation of Na-coupled solute transport triggers contraction of circumferential actomyosin fibers in the terminal web of the microvillar cytoskeletal system, thereby pulling apart junctions and allowing paracellular absorption of nutrients by solvent drag as described in the previous accompanying paper. Anatomical evidence in support of this hypothesis is presented in the following second accompanying paper.

Key Words intestinal epithelium · epithelial impedance · paracellular pathways · glucose-controlled permeability · brush-border contraction · impedance analysis

I. Introduction

The rate of absorption of fluid from the small intestine is greatly stimulated by addition of glucose or amino acids to luminal fluid [1, 19, 42, 47]. Activation of Na-coupled solute transport not only increases fluid absorption, it also increases clearances of creatinine, phenolsulfonpthalein, inulin and other inert markers added to luminal perfusion fluid [19, 42]. The clearances of these markers are dependent on rate of fluid absorption (solvent drag) as well as on molecular size. In the glucose-activated intestine of rats the clearances of inulin or of PEG_{4000} may be as large as 30% of intestinal contents per hour, thus indicating the presence of relatively large paracellular pathways, which can account for a major portion of observed transport of glucose or amino acids under normal conditions [42]. The question to be asked in the present paper is whether paracellular pathways (intercellular junctions) are under physiological control by nutrients undergoing absorption. Does the presence of glucose or of amino-acids in the lumen activate opening of intercellular junctions, perhaps by stimulating the sub-brush border circumferential actomyosin system to contract? Or can the increased clearances of luminal solutes in the presence of glucose be attributed to increased osmotic absorptive flow (solvent drag) through intercellular junctions of fixed dimensions? To answer this question I measured the impedance of perfused isolated segments of small intestine following addition of actively transported substrates such as glucose, expecting that any widening of intercellular junctions would be accompanied by decreased impedance, especially at low frequencies sensitive to resistive changes. This expectation was realized; activation of Na-coupled solute transport caused a two- to threefold decrease of impedance involving simultaneous increase of capacitance (membrane surface) and conductance (width of intercellular junctions and lateral spaces).

Use of impedance techniques to investigate epithelial permeability has been reviewed by Diamond and Machen [15] with special emphasis on the epi-

* *Present address:* Concord Field Station, Harvard University, Old Causeway Road, Bedford, MA 01730.

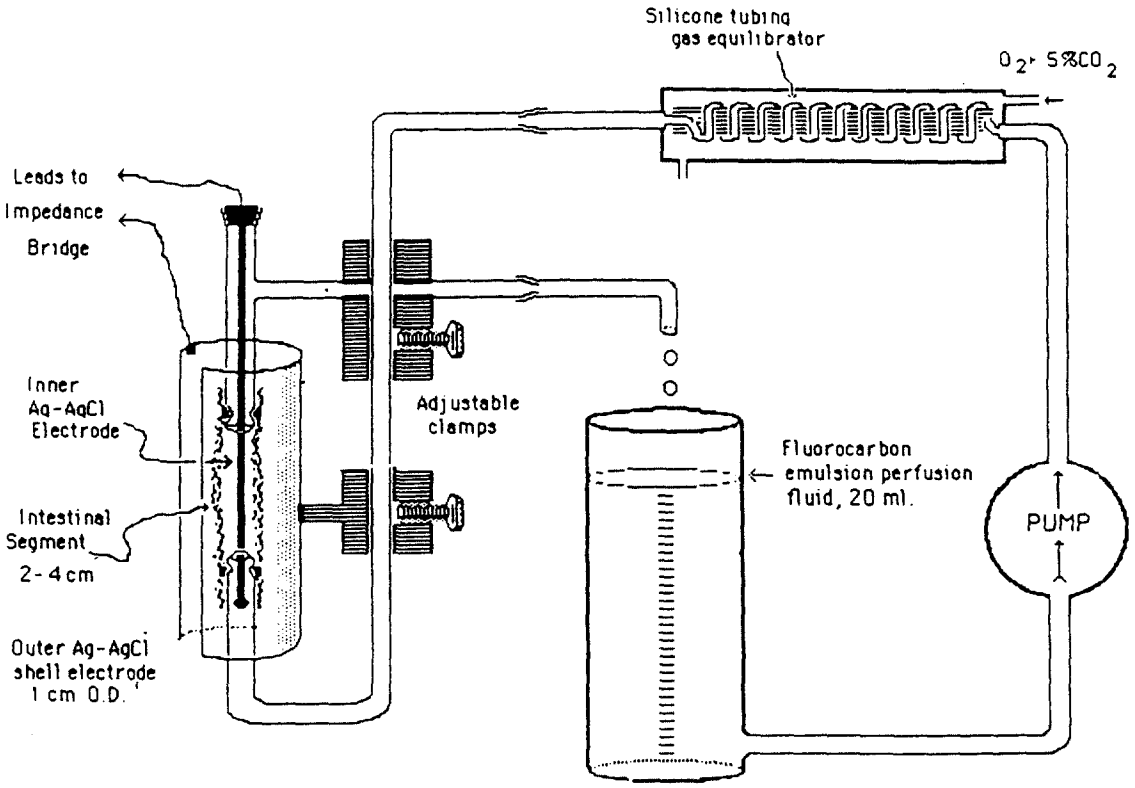

Fig. 1. Perfusion apparatus. The detachable tubular framework holding electrodes, intestinal segment and clamps was submerged in balanced, oxygenated salt solution at 38°C during perfusions. Length of segment was adjusted by upper clamp until segment was slightly stretched. Enhanced oxygen capacity from fluorocarbon emulsion was necessary to maintain viability of preparations

thelia of gall bladder and of the gastric mucosa. There have been no systematic investigations of the small intestine, although Fromm, Schulzke and Hegel [22] reported on preliminary measurements in rats. Impedance measurements as developed by Clausen, Lewis and Diamond [11] involve Bode plots in which phase angles are recorded as a function of frequency. I have employed an impedance bridge which supplies the same basic information but has practical advantages related to sensitivity and ease of measurement.

II. Materials and Methods

A. Perfusion of Isolated Segments

Intestinal segments were mounted on an adjustable tubular framework as shown in Fig. 1. The length of the perfused segment could be adjusted by a screw clamp; usually the length was set at 3.0 ± 0.5 cm with slight tension on the segment. A silver wire inner electrode was inserted through a three-way plastic stopcock to extend throughout the length of the segment; the upper part of the electrode was soldered to a male syringe fitting seated in the stopcock. A detachable silver cylindrical shell electrode with a diameter of 1 cm, a length of 4 cm and a longitudinal gap of 0.7 cm to admit the segment was mounted around the entire length of the segment. The frame holding the segment could be connected to the remainder of the apparatus within a few seconds by means of syringe fittings. During perfusion the frame with segment was submerged in balanced, oxygenated salt solution at 38°C. All submerged parts, including the clamps, were constructed of plastic except for the silver electrodes. This part of the apparatus resembled that described by Baker et al. [4].

The eccentric perfusion pump (Sigmamotor TM-20) operated on latex tubing. Approximately 20 ml of fluid were recirculated through the system at 2 ml min^{-1} via a silicone tubing gas exchanger. The silicone spirally wound tubing was 2 mm o.d., 1.65 mm i.d. and 300 cm long (volume about 6 ml).

B. Operative Procedures and Perfusion Fluids

Rats or hamsters of either sex were starved for 15 hr prior to anesthetization with 30–40 mg/kg pentothal. A 10–30 cm segment of small intestine was removed, submerged and rinsed in ice-cold 0.9% NaCl. A length of 3–4 cm was cut and mounted on the tubular frame while still immersed in the cold saline. The length was adjusted until the segment was slightly stretched. The exact length was then measured and the inner and outer electrodes placed in position as shown in Fig. 1. The entire frame with segment and electrodes was then removed from the cold salt solution, connected with the perfusion apparatus and submerged

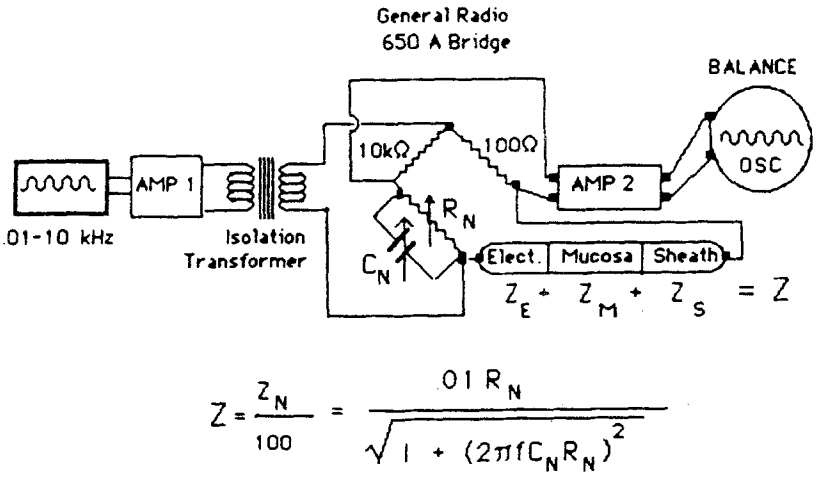

Fig. 2. Bridge circuit for impedance measurements. Reactances were balanced by R_N and C_N using oscilloscope as null indicator. Unknown impedances at any given frequency were computed from equation shown and verified as described in text

in balanced salt solution at 38°C and time zero. The operative procedures could be completed in about 10 min. Most of the segments studied were taken from midgut but all parts of the small intestine were investigated. In some segments the mucosa was removed by incubation with 5 mM EGTA, followed by extrusion of the mucosa with a roller; this procedure was important in order to determine the proportion of total impedance contributed by the mucosal epithelium alone as explained in Section A of Results. Histological examination of the segments after extrusion of the epithelium revealed that all sub-epithelial structures, including the lamina propria of individual villi, remained intact [35].

The oxygen supply to the epithelium was enhanced by addition of a fluorocarbon emulsion as described by Geyer, Monroe and Taylor [24]. This was of crucial importance because the physiological responses to be described are extremely sensitive to hypoxia (*see* Figs. 7 and 8). The composition of the perfusion fluid was NaCl, 7.25 g/liter; $NaHCO_3$, 2.1 g/liter; KCl, 0.3 g/liter; $MgCl \cdot 6H_2O$, 0.2 g/liter; $CaCl_2$, 0.22 g/liter; perfluorotributylamine (FC 43), 25 wt/vol%; Pluronic F68 stabilizer (mol wt 8350) 3.0 wt/vol%, oxygen 6 vols %, CO_2 45 mm Hg. The specific resistance at 38°C was 48 Ω-cm. 20 ml of the perfusion fluid was recirculated through the silicone gas equilibrator for several minutes before adding the $CaCl_2$ in order to prevent precipitation of carbonates. At a flow of 2 ml min^{-1} the oxygen delivery of the fluid was at least fivefold the oxygen consumption of the tissue, which maintained reversible physiological responses to glucose or to hypoxia for 1–2 hr. Professor Geyer (Harvard School of Public Health) kindly provided the fluorocarbon emulsions, which can now be obtained commercially from the Green Cross Corp., Osaka, Japan.

C. Electrical Measurements

Most of the impedances were measured with a General Radio 650 A Bridge as shown in Fig. 2. Sine waves from a Simpson Model 420 function generator were amplified and supplied to the bridge through a Model 578A General Radio isolation transformer. The voltage supplying the bridge was monitored by a capacity coupled oscilloscope. Output of the bridge was amplified and monitored by a second oscilloscope which was used as a null indicator. At frequencies below 300 Hz, a low bandpass filter was employed to reduce noise. External decade capacitors (C_N) in parallel with the variable bridge resistor, R_N, were used to adjust Z_N, to match Z in the unknown arm. Z was calculated from the values of R_N and C_N required to balance the bridge at each frequency (Equation shown in Fig. 2). The calculations were verified by substituting precision impedances for Z; accuracy was within 2% over the range 5–100 Ω. The circuit shown in Fig. 2 has recently been improved by eliminating the first amplifier and isolation transformer, grounding one side of the bridge input and using a high impedance differential amplifier (Tektronix 3A9) and oscilloscope (564B) as detector. With this circuit, impedances in the range 5–100 Ω could be measured within an accuracy of 2% at frequencies from 0.001–100 kHz. Ample sensitivity was obtained with a bridge voltage (AC) of 25 mV corresponding to about 5 mV across the epithelium. I am indebted to Mr. Paul Ruenzel for suggesting these improvements.

The inner silver wire electrode was cleaned with emory cloth and then chlorided for about 10 min at 7 mA in 0.1 N HCl. The freshly chlorided electrode was then "conditioned" by alternately using it as a cathode or anode until the resistance stabilized. These procedures were important because the impedance of the inner electrode was a significant fraction of the impedance of the intestinal segments, and it was therefore essential to work with electrodes of constant known characteristics. When treated as above the electrode impedances at frequencies ≥0.03 kHz did not vary by more than ±2 Ω per cm length from one experiment to the next or during the course of any one experiment. The impedance of the electrode-bath system (i.e., without the intestinal segments) was inversely proportional to the surface area of the inner electrode; the data shown in Fig. 3 refer to an electrode 1.62 mm in diameter having a surface area of 0.51 cm^2 per cm length. The electrode impedance was measured before and after each experiment and the electrode was freshly cleaned and chlorided whenever its impedance differed from that shown in Fig. 3 by more than 1 SD.

III. Results

A. Impedance of Electrodes and of Sub-Endothelial Tissue

As indicated in Fig. 2 the impedance of bridge arm Z consists of three impedances in series. (i) the electrodes and bathing fluids, (ii) the mucosal epithe-

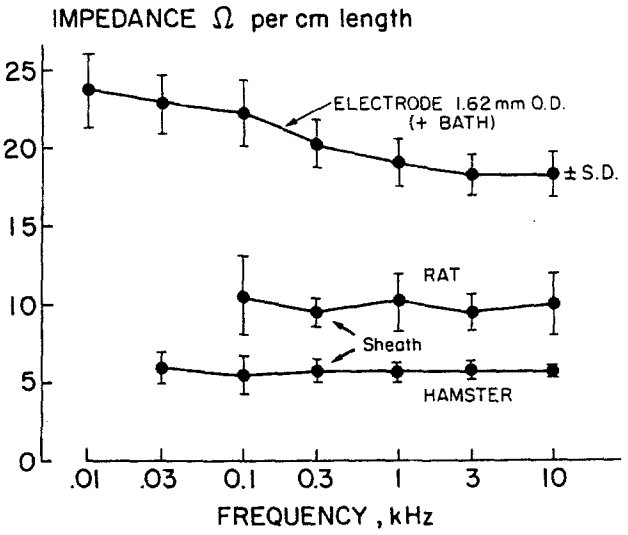

Fig. 3. Electrode and submucosal (sheath) impedances as a function of frequency. The surface area of the inner electrode was the limiting impedance for the electrode-bath component; this was shown by using inner electrodes of varying diameter (surface area). The electrode had a small reactance component as indicated by its frequency dependence. The sheath impedances were determined on segments which had been denuded of their epithelial layers by incubation in EGTA followed by extrusion of the mucosa with a roller but leaving lamina propria and smooth muscle layers intact. Impedance of sheath was primarily resistive as shown by independence of frequency; reasons for differences between rat and hamster sheath impedances are discussed in text. The *epithelial* components of impedances shown in the remainder of this paper were obtained by subtracting electrode + sheath impedances from total measured transmural impedances at each frequency

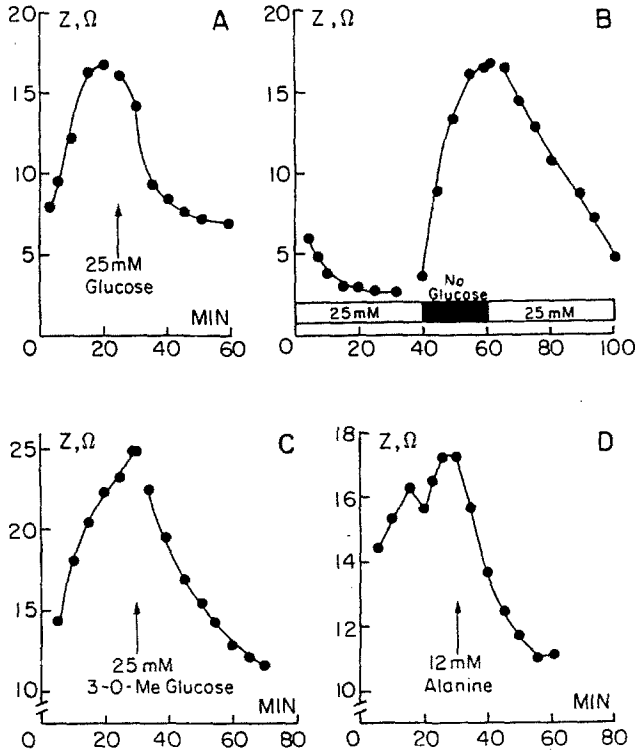

Fig. 4. Effects of glucose, 3-O-methyl glucose or alanine on impedance of mucosal epithelium at 1 kHz. Perfused small intestinal segments of rats; Z = Ω per cm length of segment. The increase of impedance prior to addition of exogenous transportable substrates in *A*, *C*, and *D* is presumably a result of depletion of residual substrate. If exogenous glucose is originally present the impedance remains constant or decreases slightly as shown in *B*. Addition of transportable organic substrates to glucose-free tissue causes prompt reduction of impedance involving both resistive and capacitative components, as explained in text

lium, which is a complex impedance as described below, and (iii) the submucosal lamina propria and smooth muscle (sheath). In order to analyze the impedance of the mucosal epithelium it is necessary to subtract from the total the sum of the electrode and sheath impedances; these are relatively constant as a function of frequency and do not take part in the physiological reactions to be described. Figure 3 shows the impedance of electrodes and sheath as a function of frequency, together with standard deviations. The sheath data refer to segments of ileum or jejunum after removal of the epithelium as described in Materials and Methods. Impedance of the electrode system (inner electrode, salt solution and outer electrode) decreases from 23.7 ± 2.0 Ω at 0.01 kHz to 17.5 ± 1.0 Ω at 30 kHz, all values being expressed per cm length of exposed electrode. When the intestinal sheath (total tissue after extrusion of epithelium) is mounted between the electrodes there is an additional 6.0 ± 0.5 (SE) Ω per cm length at all frequencies. The sheath impedance is relatively small compared to electrode impedance, and its independence of frequency indicates that it is primarily resistive. Additional control experiments showed that the sheath impedance, unlike the epithelial impedance is not altered by glucose or amino acids. In the remainder of this paper it will therefore be assumed that the mucosal epithelial impedance at any given frequency is equal to the observed total impedance minus the sum of the electrode and sheath impedances shown in Fig. 3.

The rat intestine is thicker than that of the hamster (wet wt 110 ± 4 mg per cm length for rat, 60 ± 5 mg per cm for hamster), and this is reflected in the resistance of the sheath (10 Ω/cm in rat, 6 Ω/cm in hamster). It was noted also that the mucosal epithelium is more easily detached from rat than from hamster intestine. After one or two hours of perfusion of isolated rate intestine the mucosa may be readily extruded with a roller without incubation with EGTA; some sloughing may even occur during perfusion in vivo with intact blood supply. For this

reason hamsters are more suitable than rats for anatomical studies of intestinal epithelium, especially following in vitro studies. Perhaps it is for this reason, also, that everted sac preparations of the hamster are more viable than those from rats [31]. Nevertheless, the changes of epithelial impedance initiated by Na-coupled solute transport are as large in the rat as they are in hamsters, as will be shown below.

B. Effects of Na-Coupled Solute Transport on Impedance of the Intestinal Mucosa: Results and Interpretations

Figure 4 illustrates the effects of adding small amounts of glucose, 3-O-Me-glucose or alanine on impedance of rat small intestine, measured at 1 kHz. When the cold intestinal segments are first exposed to the warm perfusion fluid at zero time in the absence of substrate, the impedance is low but it gradually increases to a high constant value in 15–30 min at 38°C (Fig. 4*A*, *C*, *D*). This behavior is similar to that described by Baker et al. [4]. Addition of glucose, 3-O-Me-Glucose or alanine brings about prompt reduction of impedance to its original low level or below. However, if glucose is originally present in perfusate the impedance remains at its initial level or below (Fig. 4*B*). It seems probable, therefore, that the initial low impedance in the absence of added substrate can be accounted for by a small residual store of glucose in the tissue; the impedance then increases as the store is depleted by metabolism. This interpretation is supported quantitatively by the following calculation: (i) the glucose metabolism of isolated intestinal segments is about 20 μmol hr^{-1} per g wet wt [30]; (ii) the amount of glucose in the tissue fluids at the time of excision is 5–10 μmol per g (corresponding to 5 mM in plasma). Tissue stores are therefore sufficient to last for 15–30 min, and this corresponds to the observed duration of increase of impedance following exposure of the tissue to substrate-free perfusion fluid (Fig. 4*A*, *C*, *D*). The importance of this 15-min store of glucose for interpretation of the effects of glucose on fluid absorption in isolated everted sacs has been pointed out in the preceding paper (paragraph 5 of Discussion [42]).

The changes of impedance shown in Fig. 4 were accompanied by changes of capacitance as indicated by changes of C_N required to balance the bridge (*see* Fig. 2, Materials and Methods). The directional changes of C_N indicated that the capacitative reactance of the intestine was decreased by Na-coupled transport, but little could be learned quantitatively from measurements at a single frequency. The measurements were therefore extended to cover a wide range of frequencies in the steady state.

Figure 5*A* and *B* show steady-state impedances as a function of frequency in the presence or absence of 10–25 mM glucose in hamster and rat intestine. Figure 5*C* and *D* show similar data for 10 mM alanine or leucine. It is clear that these transportable substrates bring about very large decreases of transepithelial impedance. Interpretation of Fig. 5 in terms of capacitative and resistive components of impedance may best be explained with the aid of a model or diagram as shown in Fig. 6. This model is similar to the "distributed resistance" models proposed for gall bladder, rabbit urinary bladder or gastric mucosa [*see* Diamond and Machen [15] for review]. As applied to the small intestine, however, the model may be simplified as in Fig. 6 because the junctional resistances are only about 10% of the parallel cell membrane resistances so that the latter may be neglected (*see* legend to Fig. 6). Under these conditions the model permits solution for the resistance of the junctions, R_J, the distributed resistance of lateral intercellular spaces, R_L, and the lumped capacitance, C_M, of the microvilli in series with the distributed capacitance of the basolateral surfaces of the epithelial cells. The lumped capacitance, C_M, provides no direct information as to which of the cell surfaces change during Na-coupled solute transport. However, supplementary information from anatomical data indicates that the capacitance of the apical microvilli is so large that observed values are determined primarily by the basolateral surfaces (C_{BL}) as discussed below. Analytical solution for the circuit of Fig. 6 has been presented by K.S. Cole [12] in the form

$$Z = \sqrt{\frac{Z_0^2 + \{2\pi f(Z_0 - Z_\infty)C_M Z_\infty \times 10^{-3}\}^2}{1 + \{2\pi f(Z_0 - Z_\infty)C_M \times 10^{-3}\}^2}}. \qquad (1)$$

Equation (1) fits the analog RC circuit shown in Fig. 6 within 2% as measured on our apparatus. As applied to the experimental data of Fig. 5 the value of Z_0 at low frequencies is taken to be equivalent to $R_J + R_L$ and the value of Z_∞ at high frequencies is taken to be equivalent to R_L. The value of C_M is taken as that which gives the best fit to the data for the indicated values of Z_0 and Z_∞. The solid lines shown in Fig. 5 are *theoretical* curves predicted by Eq. (1) using the analog model of Fig. 6 and the values of R_J, R_L and C_M shown on the panels. The experimental values tend to be slightly lower than theoretical in the range 0.1–1 kC and slightly higher in the range of 1–10 kC. Recent measurements (not to be considered further in this paper) show that

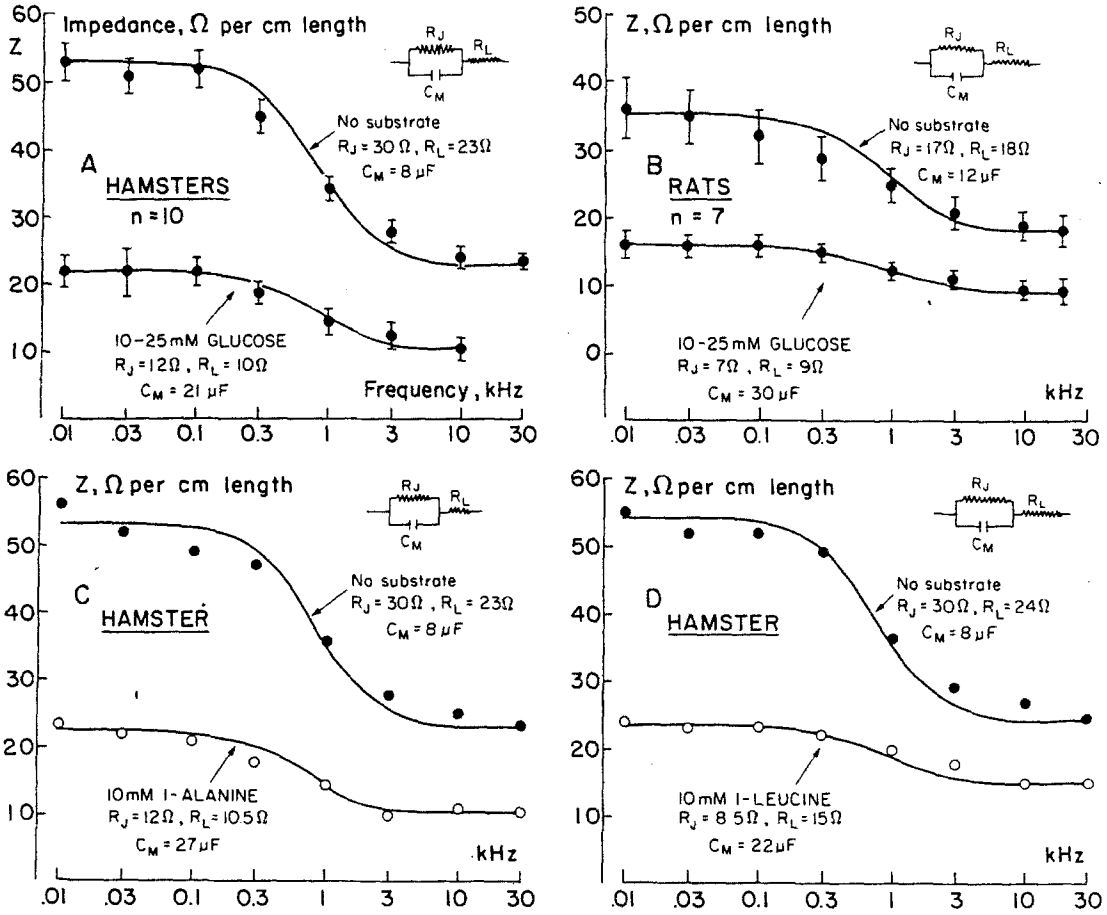

Fig. 5. Steady-state impedances as a function of frequency with and without transportable substrates. (*A*) Effects of glucose in hamsters, means ± SE. (*B*) Effects of glucose in rats, means ± SE. (*C*) Effects of alanine, example of one experiment. (*D*) Effects of leucine, example of one experiment. The solid lines are *theoretical* curves predicted by Eq. (1) using the analog model and values of R_J, R_L and C_M shown in the inserts (*see also* Fig. 6). The experimental values are slightly lower than theoretical in the range 0.1–1 kHz and slightly higher in the range 1–10 kHz, thus indicating that the model describes the system well, but not exactly

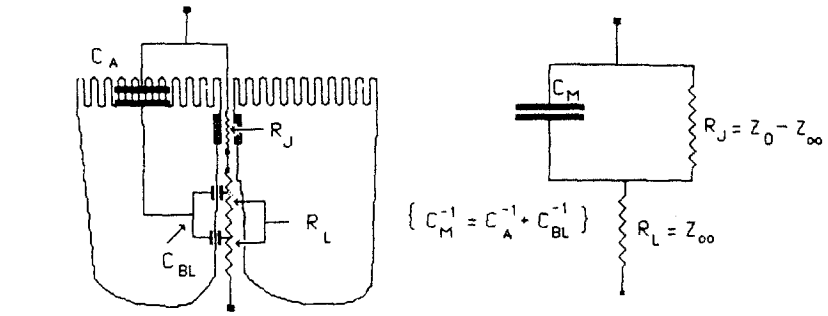

$$Z = \sqrt{\frac{Z_0^2 + [2\pi f(Z_0 - Z_\infty) C_M Z_\infty \times 10^{-3}]^2}{1 + [2\pi f(Z_0 - Z_\infty) C_M \times 10^{-3}]^2}}$$

Z, R -- Ω
C -- μF
f -- kHz

or

$$C_M = \frac{159}{(Z_0 - Z_\infty) f} \sqrt{\frac{Z_0^2 - Z^2}{Z^2 - Z_\infty^2}}$$

Fig. 6. Electrical analog of epithelial impedance in small intestine. This model is similar to the "distributed resistance" model of Frömter [23] and others (*see* [15] for review). As applied to the small intestine the intercellular junctional resistance, R_J, is only about 10% of the parallel plasma membrane resistance, so the latter can be neglected. Thus plasma membrane resistances are of the order of 2000–4000 Ω per μF [7, 23], whereas junctional resistances are in the range 200–400 Ω per μF as shown in the present paper. The frequency-impedance function of the model matches closely the relations between frequency and impedance measured experimentally in perfused intestinal segments under a variety of conditions as illustrated in Figs. 5 and 8. Other, more complex, models might fit the data equally well, but this figure represents the simplest model in which the resistances and capacitances are interpretable in terms of measured permeabilities to inert solutes and measured surface areas of epithelial membranes

impedance continues to decrease slightly in the range 10–100 kHz, thus suggesting that at high frequencies a greater proportion of current traverses basal membranes, bypassing the lateral spaces and effectively reducing the distributed resistance, R_L. However, the simplified equivalent circuit shown in Fig. 6 and described by Eq. (1) fits experimental data in the range 0.01–10 kHz with sufficient accuracy for purposes of the present paper. Figure 6 may be explained qualitatively as follows: (i) At low frequencies (0.01–0.03 kHz) the impedance, Z, of the lipid plasma membranes is so large compared with that of the paracellular channels that almost all the current passes through $R_J + R_L$ in series; (ii) at high frequencies (3–10 kHz) the impedances of apical and lateral cell membranes (in series) are so low relative to R_J that R_L becomes the limiting impedance, Z_∞; (iii) at intermediate frequencies the measured impedance, Z, is determined by the capacitance of apical and lateral plasma membranes in accordance with Eq. (1). The impedance changes illustrated in Fig. 5 are characteristic of all parts of the small intestine from the duodenum to the lower ileum. In contrast, the frequency-impedance function of epithelium from large intestine does not fit the simple model shown in Figs. 5 and 6 and glucose has little or no effect on the impedance at any frequency.

Discussion and further experimental results relating specifically to Fig. 5 are presented below under specific headings, leaving general theory for the final discussion section.

1. Comparison with Previous Measurements of Intestinal Transmural Resistance

It is well known that glucose increases the transmural potential difference and short-circuit current, but the large changes in resistance and capacitance shown in Fig. 5 have been overlooked. Table 1 summarizes results obtained by previous investigators using various preparations of the intestine. In order to compare the results shown in Fig. 5 with those of Table 1 it is necessary to express results in Ω per cm^2 of serosal area and to add back the sheath resistances which were included in most previous investigations. Thus from Fig. 5*B* (rat) $R_T = R_J + R_L + R_{sheath} = 17 + 17 + 10 = 44$ Ω per cm length. Each cm length of rat intestine has a serosal surface area of 2 cm^2 [20, 42], whence total transmural resistance at low frequency in the glucose-free state is 88 Ω cm^2 as shown in Table 1. The corresponding figure for the hamster (from Fig. 5*A*) is 122 Ω cm^2.

Inspection of Table 1 indicates that transmural resistances of flat sheets of intestine mounted in Ussing-type chambers are about the same with or without glucose. The only exceptions are the measurements of Munck [37]. In contrast, the D.C. transmural resistances reported by Clarkson [9] and by Baker et al. [4] for glucose-free segments and by Barry et al. [5] for glucose-activated segments agree well with the low frequency impedances found in the present work on perfused segments with and without glucose. Munck [37] noted that the glucose response in his flat sheet preparations was vulnerable to hypoxia and suggested that ". . . the very marked differences between the electrical characteristics of the Ussing and the sac preparations of rat jejunum might be explained by different degrees of tissue oxygenation." In the flat mounted preparations listed in Table 1 the exposed areas of mucosa were all less than 1.5 cm^2 and some were as small as 0.2 cm^2. It is therefore likely that edge damage, variable degrees of stretch and uncertain oxygen supply (no fluorocarbon enrichment) contributed to the failure of such preparations to respond to glucose in the manner described in the present paper. In an accompanying paper [35] we show that the ultrastructural changes associated with the glucose response occur in intact, blood circulated intestinal epithelium of anesthetized hamsters as well as in fluorocarbon perfused segments,

Table 1. Effects of glucose on transmural resistance of small intestine. Ω per cm^2 serosa

Tissue	No glucose	Glucose	Reference
Flat sheets between two compartments, 0.2–1.5 cm^2 serosal area			
Rat midgut	—	63	Asano [3]
Rabbit ileum	66	66	Schultz, Zalusky [45]
Rabbit ileum	89	—	Field et al. [18]
Rat jejunum	66	37	Munck [37]
Rabbit ileum	100	—	Frizzell, Schultz [21]
Rat jejunum	—	99	Feldman et al. [17]
Goldfish midgut	106	106	Albus, v. Heukelom [2]
Rat jejeunum	44	44	Munck, Schultz [38]
Rat jejeunum	66	65	Okada et al. [39]
Rat ileum	90	86	Okada et al. [39]
Rat jejeunum	47	—	Fromm et al. [22]
Guinea pig midgut	—	50–57	Madara et al. [34]
Segments or sacs 5–16 cm^2 serosal area			
Rat ileum	78	—	Clarkson [9]
Rat midgut	—	29	Barry et al. [5]
Rat jejunum	110	—	Baker et al. [4]
(everted)	55	—	
Rat midgut	88	54	Present
Hamster midgut	122	58	Present

whereas they do not occur in flat sheets mounted in Ussing-type chambers of small aperture.

2. *Membrane Capacitance and Surface Area*

The capacitance of glucose-free midgut is 8 μF per cm length in the hamster and 12 μF in the rat (Fig. 5). The histological surface area of the villi in fixed tissue is in the range 4.5 to 7.5 cm^2 per cm length in rats [20] and 8 cm^2 in hamsters [35]. Since the capacitance of most cell membranes (lipid bilayer) is about 1 μF per cm^2 cell surface, the results shown in Fig. 5 indicate that the cell surfaces which determine the lumped capacitance are 1–2 × the histological surface of the villi. It is probable, however, that the functional area of the microvilli at the apical surface far exceeds the histological area because the spaces between microvilli are easily accessible to solutes as large as horse radish peroxidase [32]. Therefore the capacitative reactance is determined primarily by the distributed capacitance of the basolateral surfaces (C_{BL} in Fig. 6) and the 2.5-fold increase of capacitance associated with Na-coupled solute transport results from widening of intercellular spaces with concomittant exposure of lateral surfaces. From the relations between C_M, C_A and C_{BL} (Fig. 6) it follows that a three- to fourfold increase in surface area of basolateral surfaces would account for the observed 2.5-fold increase of C_M if the functional surface of the apical microvilli were 60–120 cm^2 (μF) per cm length or 10–20 × the histological surface of the villi. In an accompanying paper [35] we show that activation of Na-coupled transport does in fact expand the intercellular spaces and increase the exposed surface area of lateral membranes without detectable changes in the geometry of microvilli.

3. *The Absolute Value of Junctional Resistance: Calculation of Area per Unit Path Length*

In the glucose-activated intestine the junctional resistance is 13 Ω per cm length in hamsters and 7 Ω in rats. If the specific resistance of fluid in the junctions is the same as in perfusion fluid (48 Ω-cm at 38°C) then the area per unit path length $Ap/\Delta x$ in the junction is 48/13 = 3.7 cm in the hamster and 48/7 = 6.8 in the rat. $Ap/\Delta x$ calculated from the coefficient of osmotic flow and permeabilities to inert solutes is 4.3 cm in rat small intestine perfused in vivo [42]. Thus from permeability to inert solutes it is possible to predict with reasonable accuracy the electrical resistance of the intercellular junctions.

The path-length, Δx, through intercellular junctions is of the order of 10^{-4} cm [10] and the histological surface of the villi is about 5 cm^2 per cm length [20]. Therefore the functional cross-sectional area of the intercellular junctions is about 0.01% of the histological surface of the villi. This small area is sufficient to account quantitatively for the observed hydrodynamic and electrical resistance as well as the permeabilities to inert molecules. Approximately the same ratio of intercellular junctional area to histological area is found in the endothelium of peripheral capillaries [40, 41].

$Ap/\Delta x$ for the lateral interspaces cannot be estimated from R_L, partly because R_L is a virtual "distributed" quantity and partly because active transport of Na^+ into the lateral space alters the specific resistance by an unknown amount.

4. *Is the Decrease of Epithelial Impedance Following Addition of Glucose or Amino Acids a Result of Passive Widening of Intercellular Channels Secondary to Increased Osmotic Flow?*

It is well known that lateral spaces in epithelia of renal proximal tubules [7, 44] or gall bladder [6, 46] become distended during high rates of fluid absorption. Distension of lateral spaces following addition of glucose to our preparations is easily seen by light microscopy [35] and is manifested functionally by the decrease of distributed lateral resistance, R_L, shown in Fig. 5. Such changes might be brought about by increased intercellular hydrostatic pressure secondary to increased fluid flow through the channels. This hypothesis was tested by adding glucose in the presence of 10 mM ferrocyanide which prevents absorption of fluid by its osmotic effect as shown in Fig. 1 and 2 of an accompanying paper [42]. Results of this experiment are summarized in Table 2 and show that the presence of ferrocyanide fails to block the large changes of resistance and capacitance induced by glucose. Conversely, addition of ferrocyanide in the presence of glucose failed to cause an increase of impedance. These experiments indicate that the changes of transepithelial impedance brought about by glucose are not a passive secondary result of increased fluid absorption. Evidence that the phenomenon is an active contractile process under physiological control is presented in an accompanying paper [35].

C. Dependence of Impedance on Glucose Concentration

Steady-state values of junctional resistance, R_j, distributed lateral space resistance, R_L, and capaci-

Table 2. Effects of ferrocyanide (ferro) on the impedance response to glucose

Components of impedance per cm length	Segment A (perfused with 10 mM ferro)		Segment B (perfused with 25 mM glucose)	
	No glucose	25 mM glucose	No ferro	10 mM ferro
R_J (Ω)	38	11.5	13	10
R_L (Ω)	20	10.5	9	6
C_M (μF)	6	15	28	27

Table 3. Regulation of transepithelial resistance and capacitance by glucose[a]

Luminal glucose (mM)	Junctional resistance R_J (Ω)	Lateral space resistance R_L (Ω)	Distributed capacitance C_M (μF)
0	35 ± 3	24 ± 3	8 ± 1
1.0 ± 0.05	25 ± 2	22 ± 3	10 ± 2
2.7 ± 0.2	17 ± 1	16 ± 2	19 ± 4
4.9 ± 0.4	14 ± 1	12 ± 2	25 ± 6
25 ± 5	15 ± 1	10 ± 1	25 ± 3

[a] Steady-state values per cm length, means ± SE, hamster intestine

tance, C_M, as a function of luminal glucose concentration are shown in Table 3. For these experiments the perfusion fluid contained normal salts, 12.5 wt/vol% fluorocarbon emulsion and about 1, 3 or 5 mM glucose. The volume of perfusion fluid was increased to 40 ml in order to minimize losses of glucose due to metabolism; glucose concentration was measured by glucose oxidase in samples taken at the middle of each 20–30 min steady-state period. Results summarized in Table 3 show that the half-maximal effect of glucose on transepithelial impedance occurs at a concentration of about 3 mM, which is close to the K_m of glucose transport in intestinal epithelia [13] and in epithelial vesicles [16]. This result strengthens the view that the impedance change is linked to activation of Na-coupled transport of organic solutes.

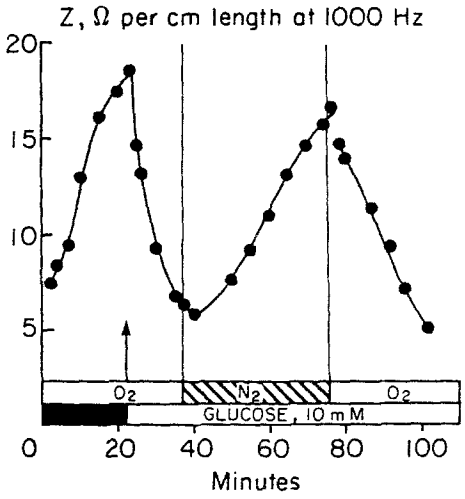

Fig. 7. Effects of hypoxia on impedance of intestinal epithelium, rat midgut. Addition of 10 mM glucose in the presence of oxygen (at 21 min) caused the usual decrease of impedance. Exposure to hypoxia (at 40 min) caused impedance to increase almost threefold even though perfusion with glucose was maintained. The effect was fully reversible when oxygen was restored at 77 min

D. Dependence of Physiological Regulation of Impedance on Oxygen Supply

Figure 7 shows the (reversible) effects of exposing the perfusion fluid to 94 ± 1% N_2 + CO_2 instead of 95% O_2 + CO_2. Addition of 10 mM glucose (at 21 min) to the glucose depleted, oxygenated segment caused the usual decrease of impedance, in this case from 18.5 to 5.8 Ω per cm length. When N_2 was substituted for O_2 in the gas equilibrator (at 40 min) the impedance gradually increased to 17.5 Ω despite continued perfusion with glucose. Restoration of the oxygen supply (at 77 min) caused return of the impedance to 5.2 Ω.

Figure 8 shows impedance-frequency plots in hamster small intestine (midgut) in the presence of glucose before and after exposure of the gas exchanger to 94% N_2 + CO_2. It is clear that the effects of glucose on the capacitance (surface area) and resistance (intercellular junctions and lateral spaces) are dependent on an adequate oxygen supply. Intermediate degrees of hypoxia were not investigated systematically, but the gradual changes of impedances observed during exposure to nitrogen and subsequent recovery on oxygen (Fig. 7) indicate that intermediate states of impedance exist as a function of oxygen pressure. If the epithelium is exposed to a fully de-oxygenated fluid for more than a few minutes the normal impedance cannot be restored following re-admission of oxygen to the system.

E. Possible Role of Ca^{2+} in the Impedance Response to Glucose

An increase in intracellular Ca^{2+} triggers opening of junctions between epithelial cells in cultured mono-

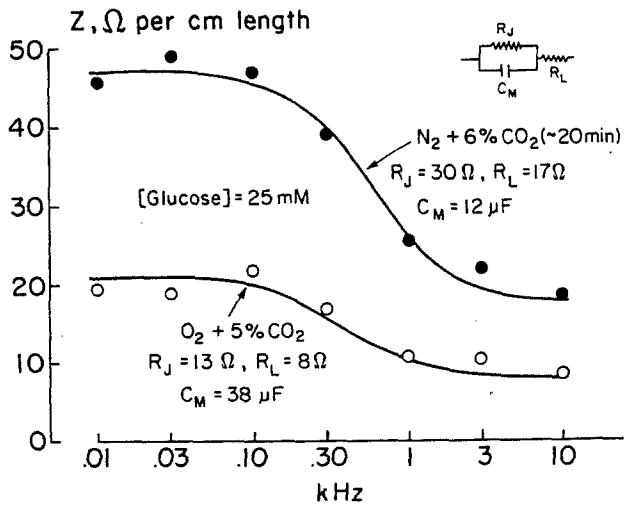

Fig. 8. Effects of hypoxia on the impedance-frequency function in the presence of glucose, hamster midgut. Data for the nitrogen curve were obtained about 20 min after substituting nitrogen for oxygen in the gas exchanger; during the equilibration period the tissue was exposed to steadily decreasing oxygen pressures (not measured). If the epithelium is exposed to fully de-oxygenated perfusion fluid it deteriorates after a few minutes as indicated by failure to recover normal impedance following re-admission of oxygen. The anatomical concommitants of hypoxia corresponding to the impedance changes are described in an accompanying paper [35]

layers [8] and between endothelial cells of small venules [14]. A calcium transport system in basolateral membranes of rat intestinal epithelium has been described [26] and contraction of sub-brush border actomyosin requires ATP and either Ca^{2+} [28] or Mg^{2+} [43]. It is therefore reasonable to suppose that activation of Na-coupled solute transport might increase intracellular Ca^{2+}, thus triggering contraction of circumferential actomyosin and opening zonnulae occludens. However, the following experiments, each repeated at least once, failed to demonstrate a link between the glucose response and entrance of Ca^{2+} into the cells. (i) 50 mM KCl in the mucosal perfusion fluid failed to alter the impedance although the normal response to glucose could be elicited after 30 minutes of perfusion with the high KCl. (ii) Normal glucose responses were obtained from segments perfused and bathed with Ca^{2+}-free solutions to which 100 μM EGTA had been added to remove traces of Ca^{2+} which might have contaminated the doubly distilled water used routinely for preparation of perfusion fluids. (iii) Nifedipine (5–50 μM) failed to block the glucose response in the presence of normal Ca^{2+}, although there was some evidence that Nifedipine can block the glucose response in segments perfused with calcium-free solutions. (iv) The Ca^{2+} ionophore A23187 (5 μM) or the dihydropyridine Ca^{2+} channel agonist PN202-791 [25] failed to cause an impedance change in the absence of glucose.

These results do not support the hypothesis that changes of impedance induced by Na-coupled solute transport are triggered by entrance of extracellular Ca^{2+} into the cells to activate contraction of perijunctional actomyosin.

IV. Discussion

A. General

It was proposed in the previous (accompanying) paper that a major fraction of intestinal absorption of nutrients normally takes place by solvent drag through intercellular junctions. In theory, this could occur through junctions of fixed dimensions at a rate proportional to fluid absorption; the only effect of glucose or other actively transported substrate would be to stimulate the rate of fluid absorption. Alternatively, or additionally, it is possible that Na-coupled solute transport might trigger a mechanism which increases the width of intercellular junctions, thus increasing passive absorption of nutrients by solvent drag at any given rate of fluid absorption. Such a mechanism would be teleologically sound because the presence of products of digestion in the intestine would amplify the absorptive process, thus providing positive feedback in its literal, as well as its theoretical, sense.

Results of the impedance measurements described in the present paper leave little doubt that dimensions of paracellular pathways, including junctions, can be regulated by the concentration of normal products of digestion such as glucose or amino acids. The fact that large decreases of impedance are initiated by 3-O-methyl glucose as well as by glucose and amino acids indicates that the phenomenon is linked to Na-coupled solute transport in general. This conclusion is strengthened by the finding that half-maximal effects on impedance occur near the K_m for glucose transport (Table 3). It has been suggested that the low transmural resistance of the intestine might be explained by desquamation of cells at the tips of the villi which could conceivably leave temporary gaps or leaks. The fact that $Ap/\Delta x$ varies quickly and reversibly over a fourfold range as a function of glucose or oxygen concentration argues strongly against this hypothesis.

B. On the Link Between Na-Coupled Solute Transport and Opening of Intercellular Junctions

The magnitude of the changes in transepithelial resistance and capacitance following addition of

transportable substrates indicates that the response involves large changes in the width of paracellular channels and exposed surface area of epithelial cell membranes. Dependence of the response on oxygen pressure suggests that some energy-dependent contractile process may be involved. The sub-brush border region of intestinal epithelial contains a rich network of circumferential actomyosin fibers attached to the zonnulae adherens on the inner surface of the cell membrane adjacent to intercellular junctions [27] as well as to the junctions themselves [33]. As stated in a review by Mooseker [36], "The cytoskeletal apparatus which underlies and supports the apical brush border surface of the intestinal epithelial cell is among the most highly ordered arrays of actin filaments and associated proteins in nature." Isolated pieces of brush border, deprived of Ca^{2+} and ATP, contract vigorously when these components are restored to the medium [29, 43]. The reaction is inhibited by specific antibodies to sub-brush border myosin [28]. It seems reasonable to suppose, therefore, that Na-coupled solute transport triggers contraction of sub-brush border circumferential actomyosin, thereby exerting tension on the zonnulae adherens to widen intercellular junctions. Anatomical evidence in support of this hypothesis is given in the accompanying paper on structural concomittants of the impedance changes [35].

I thank Dr. James L. Madara for helpful discussions and Ms. Tanya Atagi for assistance with some of the experiments. The project was supported, in part, by a Pilot Study Grant from the Harvard Digestive Diseases Center, NIH Grant #1-P30-AM-34854.

References

1. Adibi, S.A. 1970. Leucine absorption rate and net movements of sodium and water in human jejunum. *J. Appl. Physiol.* **18:**753–757
2. Albus, H., Heukelom, J.S. van 1976. The electrophysiological characterization of glucose absorption by the goldfish intestine as compared to mammalian intestines. *Comp. Biochem. Physiol.* **54A:**113–119
3. Asano, T. 1963. Metabolic disturbances and short-circuit current across intestinal wall of rat. *Am. J. Physiol.* **207:**425–422
4. Baker, R.D., Watson, S., Long, J.L., Wall, M.J. 1969. Effects of eversion on transmural electrical properties of rat jejunum. *Biochim. Biophys. Acta* **173:**192–197
5. Barry, R.J.C., Smyth, D.H., Wright, E.M. 1965. Short circuit current and solute transfer by the rat jejunum. *J. Physiol. (London)* **181:**410–431
6. Bindslev, N., Tormey, J. McD., Wright, E.M. 1974. The effects of electrical and osmotic gradients on lateral intercellular spaces and membrane conductance in a low resistance epithelium. *J. Membrane Biol.* **19:**357–380
7. Boulpaep, E.L. 1972. Permeability changes of the proximal tubule of *Necturus* during saline loading. *Am. J. Physiol.* **22:**517–531
8. Cereijido, M., Meza, I., Martinez-Palomo, A. 1981. Occluding junctions in cultured epithelial monolayers. *Am. J. Physiol.* **240:***C*96–*C*102
9. Clarkson, T.W. 1967. The transport of salt and water across isolated rat ileum. *J. Gen. Physiol.* **50:**695–727
10. Claude, P. 1978. Morphological factors influencing transepithelial permeability: A model for the resistance of the zonnulae occludens. *J. Membrane Biol.* **39:**219–232
11. Clausen, C., Lewis, S.A., Diamond, J.M. 1979. Impedance analysis of a tight epithelium using a distributed resistance model. *Biophys. J.* **26:**291–318
12. Cole, K.S. 1968. Membranes, Ions and Impulses. Chs. 1 and 10. University of California Press, Berkley
13. Crane, R.K. 1968. Absorption of sugars. *In:* APS Handbook of Physiology. Alimentary Canal III: Intestinal Absorption. pp. 1323–1351. C.F. Code, editor. Williams & Wilkins, Washington, D.C.
14. Crone, C. 1986. Modulation of solute permeability in microvascular endothelium. *Fed. Proc.* **45:**77–83
15. Diamond, J.M., Machen, T.E. 1983. Impedance analysis in epithelia and the problem of gastric acid secretion. *J. Membrane Biol.* **72:**17–41
16. Dorando, F.C., Crane, R.K. 1984. Studies of the kinetics of Na^+ gradient-coupled glucose transport as found in brush-border membrane vesicles from rabbit jejunum. *Biochim. Biophys. Acta* **772:**273–287
17. Feldman, D.S., Rabinovitch, S., Feldman, E.B. 1975. Surfactants and bioelectric properties of rat jejunum. *Am. J. Dig. Dis.* **20:**866–870
18. Field, M., Fromm, D., McColl, I. 1971. Ion transport in rabbit ileal mucosa: I. Na and Cl fluxes and short circuit current. *Am. J. Physiol.* **220:**1388–1396
19. Fisher, R.B. 1955. The absorption of water and of some small molecules from the isolated intestine of the rat. *J. Physiol. (London)* **130:**655–664
20. Fisher, R.B., Parsons, D.S. 1957. Surface area of rat intestinal mucosa. *J. Anat.* **84:**272–282
21. Frizzell, R.A., Schultz, S.G. 1972. Ionic conductance of extracellular shunt pathway in rabbit ileum. *J. Gen. Physiol.* **59:**318–346
22. Fromm, M.M., Schulzke, J.D., Hegel, U.H. 1985. Epithelial and subepithelial contributions to transmural electrical resistance of intact rat jejeunum, in vitro. *Pfluegers Arch.* **405:**400–402
23. Fromter, E. 1972. The route of passive ion movement through the epithelium of *Necturus* gallbladder. *J. Membrane Biol.* **8:**259–301
24. Geyer, R.P., Monroe, R.C., Taylor, K. 1969. Survival of rats having red cells totally replaced with emulsified fluorocarbon. *Fed. Proc.* **27:**384
25. Hess, P., Lansman, J.B., Tsien, R.W. 1984. Different modes of Ca channel gating behaviour favoured by dihydropyridine Ca agonists and antagonists. *Nature (London)* **311:**538–544
26. Hildmann, B., Schmidt, A., Murer, H. 1982. Ca^{2+} transport across basal-lateral plasma membranes from rat small intestinal epithelial cells. *J. Membrane Biol.* **65:** 55–62
27. Hull, B.E., Staehelin, L.A. 1979. The terminal web. A reevaluation of its structure and function. *J. Cell Biol.* **81:**67–82
28. Keller, T.C.S., Conzelman, K.A., Chasan, R. 1985. Role of myosin in terminal web contraction in isolated intestinal epithelial brush borders. *J. Cell Biol.* **100:**1647–1655

29. Keller, T.C.S., Mooseker, M.S. 1982. Ca^{++}-calmodulin dependent phosphorylation of myosin and its role in brush border contraction in vitro. *J. Cell Biol.* **95**:943–959
30. Lesse, H.J., Mansford, K.R.L. 1971. The effects of insulin and insulin deficiency on the transport and metabolism of glucose by the small intestine. *J. Physiol. (London)* **212**:819–836
31. Levine, R.R., McNary, W.W., Kornguth, P.J., Leblanc, R. 1970. Histological re-evaluation of everted gut technique for studying intestinal absorption. *Eur. J. Pharmacol.* **9**:211–219
32. Madara, J.L. 1982. Cup cells: Structure and distribution of a unique class of epithelial cells in guinea pigs, rabbit and monkey small intestine. *Gastroenterology* **83**:981–994
33. Madara, J.L. 1987. Intestinal absorptive cell tight junctions are linked by cytoskeleton. *Am. J. Physiol.* **253**:C171–C175
34. Madara, J.L., Barenberg, D., Carlson, S. 1986. Effects of cytochalasin D on occluding junctions of intestinal absorptive cells: Further evidence that the cytoskeleton may influence paracellular permeability. *J. Cell Biol.* **97**:2125–2135
35. Madara, J.L., Pappenheimer, J.R. 1987. The structural basis for physiological regulation of paracellular pathways in intestinal epithelia. *J. Membrane Biol.* **100**:149–164
36. Mooseker, M.S. 1985. Organization, chemistry and assembly of the cytoskeletal apparatus of the intestinal brush border. *Annu. Rev. Cell Biol.* **1**:209–241
37. Munck, G.G. 1972. Effects of sugar and amino-acid transport on transepithelial fluxes of sodium and chloride of short circuited rat jejunum. *J. Physiol. (London)* **223**:699–717
38. Munck, B.G., Schultz, S.G. 1974. Properties of the passive conductance pathway across in vitro rat jejunum. *J. Membrane Biol.* **16**:163–174
39. Okada, Y., Irimajiri, A., Inouye, A. 1977. Electrical properties and active solute transport in rat small intestine: II. Conductive properties of transepithelial routes. *J. Membrane Biol.* **31**:221–232
40. Olesen, P., Crone, C. 1983. Electrical resistance of muscle capillary endothelium. *Biophys. J.* **42**:31–41
41. Pappenheimer, J.R. 1953. Passage of molecules through capillary walls. *Physiol. Rev.* **33**:387–423
42. Pappenheimer, J.R., Reiss, K.Z. 1987. Contribution of solvent drag through intercellular junctions to absorption of nutrients by the small intestine of the rat. *J. Membrane Biol.* **100**:123–136
43. Rodewald, R., Karnovsky, M.J. 1976. Contraction of isolated brush borders from the intestinal epithelium. *J. Cell Biol.* **70**:541–554
44. Schmidt-Nielsen, B., Davis, L.E. 1968. Fluid transport and tubular intercellular spaces in reptilian kidneys. *Science* **159**:1105–1108
45. Schultz, S.G., Zalusky, R. 1964. Ion transport in isolated rabbit ileum: I. Short circuit current and Na fluxes. *J. Gen. Physiol.* **47**:567–584
46. Smulders, A.P., Tormey, J.M.D., Wright, E.M. 1972. The effect of osmotically induced water flows on the permeability and ultrastructure of the rabbit gallbladder. *J. Membrane Biol.* **7**:164–197
47. Smyth, D.H., Taylor, C.B. 1957. Transfer of water and solutes by an in vitro intestinal preparation. *J. Physiol. (London)* **136**:632–648
48. Tormey, J. McD., Diamond, J.M. 1967. The ultrastructural route of fluid transport in rabbit gall bladder. *J. Gen. Physiol.* **50**:2031–2060

Received 11 March 1987; revised 25 August 1987